

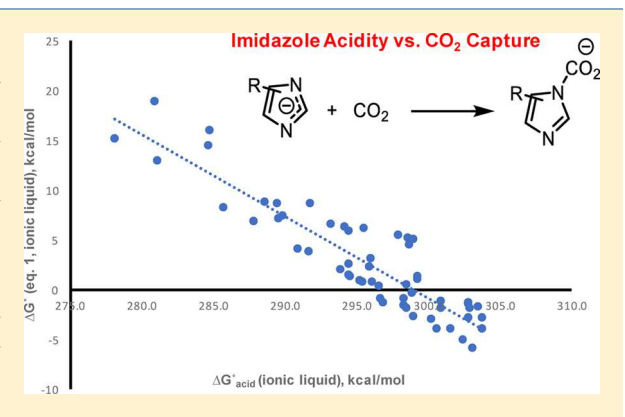
Gas-Phase and Ionic Liquid Experimental and Computational Studies of Imidazole Acidity and Carbon Dioxide Capture

Ning Wang and Jeehiun K. Lee*

Department of Chemistry and Chemical Biology, Rutgers, The State University of New Jersey, New Brunswick, New Jersey 08901 United States

Supporting Information

ABSTRACT: The capture and storage of carbon dioxide are pressing environmental concerns. Nucleophilic capture by anions in ionic liquids, such as imidazolates, is a promising strategy. Herein, the gas-phase acidity of a series of imidazoles is examined both experimentally and computationally. The intrinsic acidity of these imidazoles has not heretofore been measured; these experimental data provide a benchmark for the computational values. The relationship between imidazole acidity and carbon dioxide capture is explored computationally, both in the gas phase and in ionic liquid. The improved understanding of imidazolate properties provided herein is important for the design and development of improved systems for carbon dioxide capture.



INTRODUCTION

Fossil fuels have, for many years, been the primary source of energy worldwide. The burning of fossil fuels releases carbon dioxide, which has become an urgent environmental concern, primarily due to carbon dioxide's prominence as a greenhouse gas and related implications for climate change. The development of strategies to capture and store carbon dioxide is therefore a pressing research area.

In recent years, ionic liquids (ILs) have come to the forefront as an effective means of trapping carbon dioxide. 1-9 ILs have various advantages, including low vapor pressure, high thermal stability, lack of flammability, property tunability, and a high solvent capacity.1 Early IL studies focused on the physical absorption of carbon dioxide; this method, however, was found to be limited by insufficient carbon dioxide absorption capacity, as the partial pressure and solubility of carbon dioxide is low post-combustion.¹⁰

To overcome this limitation, researchers turned to the development of "active site-containing" ILs. Such ILs contain a functionality that will chemically react with carbon dioxide, thus effecting chemical (as opposed to physical) CO₂ absorption. Davis and co-workers developed the first of this kind in which a primary amine was covalently tethered to the imidazolium cation of the ionic liquid.²

One drawback of such amino-functionalized ILs is a large increase in viscosity after carbon dioxide absorption, which has been attributed to a strong hydrogen-bonded network. 11-14 This increase in viscosity renders such ILs less practical. This issue led to the search for "amino-free functionalized ILs" to improve carbon dioxide chemical absorption. Prominent within this type of IL are azolate ILs, which are also called aprotic heterocyclic anion (AHA) ILs. 1,13,15-18 Dai and Wang

introduced this concept with a series of ILs that paired superbases such as 1,3,4,6,7,8-hexahydro-1-methyl-2Hpyrimido[1,2-a]pyrimidine (MTBD) and trihexyl(tetradecyl)phosphonium hydroxide ([P66614][OH]) with weak nitrogen acids such as imidazole, pyrazole, triazoles, tetrazoles, and indoles. 13,15 In these AHA ILs, the anionic moiety (such as an imidazolate) nucleophilically attacks the carbon dioxide. Studies to date indicate that the basicity of the anion is important for carbon dioxide capture, capacity, and solubility, while the effect of the countercation identity is weaker. 1,13,15,15 Therefore, tuning the basicity is a key component for achieving effective CO₂ capture. 1,20-31

Herein, we use computational and experimental methods to examine the acidity of 56 imidazoles toward better understanding their properties. We also calculate the energetics associated with imidazolate and carbon dioxide complexation. The experimental measurements provide valuable data to benchmark computations and lend insight into the inherent reactivity of these species. Gas-phase measurements are complemented by gas-phase and solution-phase calculations. We aim to achieve predictive power for such properties, which would allow for more facile tunability of potential ILs for carbon dioxide capture.

RESULTS AND DISCUSSION

Acidity. Gas-Phase Acidity: Calculations. Fifty-six imidazoles were examined computationally. Figure 1 depicts the imidazoles examined. Note that for the imidazoles, 4- and 5substituted structures are tautomers. For benzimidazoles, the

Received: August 10, 2019



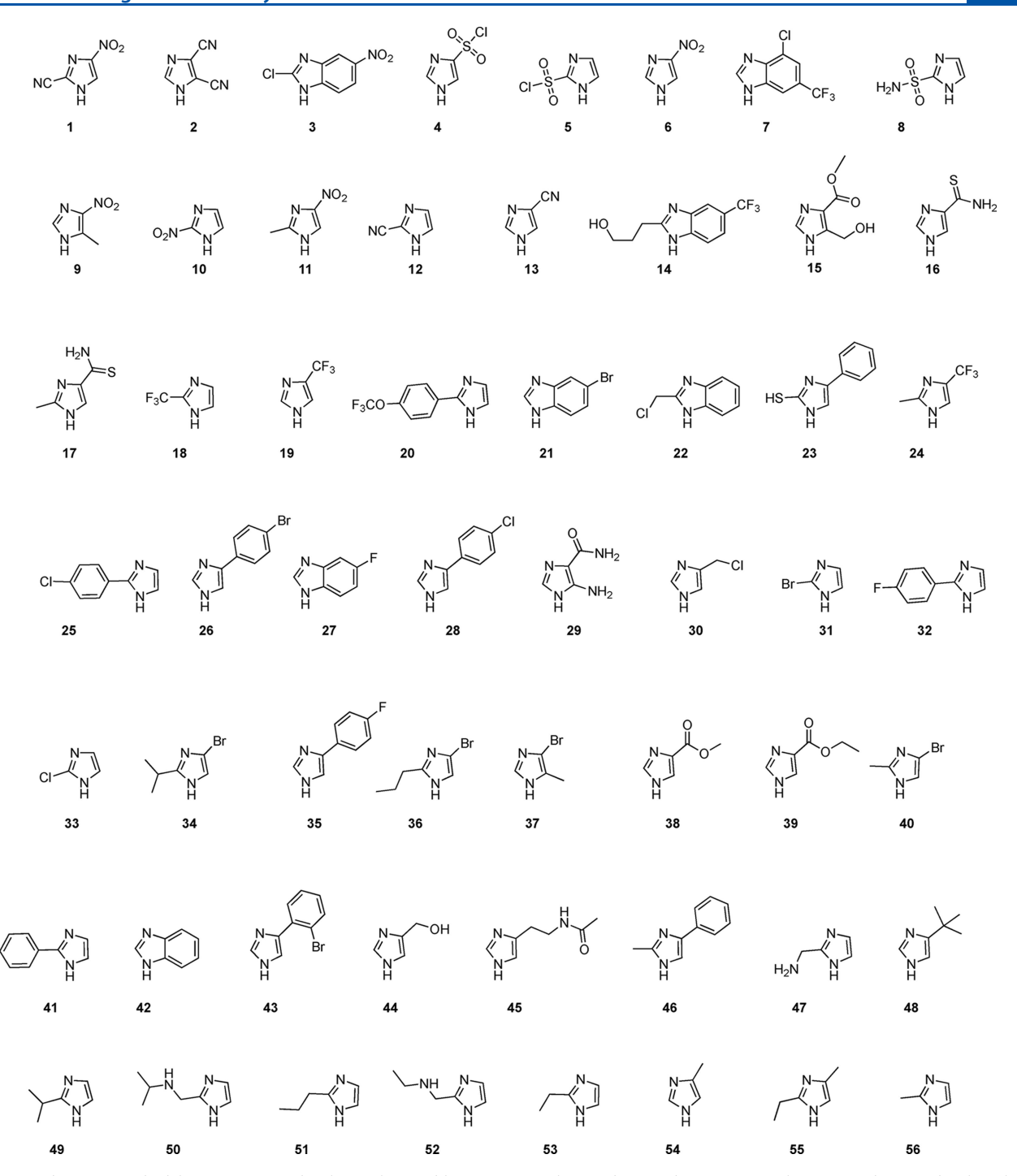


Figure 1. Substrates studied herein. For imidazoles with possible tautomers, the 4-substituted structure is shown. For benzimidazoles, the 5-substituted structure is shown. The structures are ordered by increasing calculated gas-phase acidity value.

5- and 6-substituted structures are tautomers. In Figure 1, the 4-substituted imidazoles and the 5-substituted benzimidazoles are shown.

In Table 1, the calculated gas-phase acidities of the 56 imidazoles, using B3LYP/6-311++G(d,p), are tabulated. The last column lists $\Delta G^{\circ}_{\rm rxn}$ values, which will be discussed later). Both $\Delta H^{\circ}_{\rm acid}$ and $\Delta G^{\circ}_{\rm acid}$ values are shown; the substrates in Figure 1 are ordered in decreasing acidity. The $\Delta H^{\circ}_{\rm acid}$ is the enthalpy associated with the deprotonation of the imidazole HA, and the $\Delta G^{\circ}_{\rm acid}$ is the free energy associated with the deprotonation of the imidazole HA (Scheme 1).

For those imidazoles for which there is more than one tautomer, no "prime" mark next to the structure indicates that the most stable tautomer AH is the 4-substituted imidazole or 5-substituted benzimidazole (the structures shown in Figure 1). A "prime" (′) next to the structure number indicates that the most stable tautomer AH is the 5-substituted imidazole or the 6-substituted benzimidazole.³³

Overall, the acidity trends are as one might expect; substrates with electron-withdrawing groups (for example, -NO₂, -CN, and -X where X is a halide) are more acidic. For example, the series 4, 6′, 13, 19, and 54 are all 4/5-substituted imidazoles, with, respectively, substituents -SO₂Cl, -NO₂,

Table 1. Gas-Phase Calculations (B3LYP/6-311++G(d,p)) on 56 Substrates

		(-, (-, F))						
substrate	acidity, $\Delta H^{\circ}_{ m acid}$ (kcal/mol)	acidity, $\Delta G^{\circ}_{ m acid}$ (kcal/mol)	$\Delta G^{\circ}_{ m rxn}$, ${ m CO_2}$ addition, $({ m kcal/mol})^a$	substrate	acidity, $\Delta H^{\circ}_{ m acid}$ (kcal/mol)	acidity, $\Delta G^{\circ}_{ m acid}$ (kcal/mol)	ΔG°_{rxn} , CO_2 addition, $\left(kcal/mol \right)^a$		
1	306.7	299.4	3.5	33	338.4	330.8	3.7		
2	311.4	304.0	3.3	34	338.7	331.2	0.3		
3′	315.9	308.6	3.0	35	338.8	331.9	-2.8		
4	317.2	309.5	6.7	36	339.2	331.7	-0.4		
5	317.6	309.9	10.2	37	339.7	331.8	-1.4		
6′	324.5	316.9	3.1	38′	339.8	332.2	-1.2		
7	324.7	317.3	3.6	39′	340.0	332.5	-1.2		
8	325.0	317.5	8.1	40	340.2	332.4	-1.2		
9	325.4	318.2	4.5	41	340.8	333.9	5.1		
10	326.2	318.5	2.4	42	341.0	333.5	-2.4		
11'	326.8	319.6	2.4	43′	341.6	334.0	-2.3		
12	328.7	321.3	6.2	44′	341.7	334.1	-0.4		
13	328.8	321.3	0.8	45	341.8	334.4	-5.1		
14^{b}	330.8	323.3	4.0	46	342.2	335.0	-1.8		
15	331.5	324.9	1.6	47	348.2	340.0	-5.6		
16	332.3	324.4	1.1	48	348.9	341.2	-7.3		
17	333.1	326.2	2.2	49	349.1	342.4	-4.8		
18	333.2	325.7	7.2	50	349.6	341.7	-4.5		
19	333.6	325.9	-1.1	51	349.7	342.0	-4.9		
20	333.9	327.0	6.4	52	349.9	342.0	-4.7		
21'	334.0	326.5	0.2	53	350.0	342.3	-6.5		
22	334.6	327.2	5.1	54	350.9	343.3	-8.4		
23	334.7	327.7	-1.1	55	351.1	343.9	-5.7		
24	335.5	327.7	0.2	56	351.1	343.3	-6.5		
25	336.3	330.8	4.6						
26	336.5	329.3	-1.7						
2 7′	336.7	329.2	-1.1		2	,	4-substituted or 5-		
28	337.1	329.8	-1.9				substituted product as		
29	337.4	330.3	-4.3				re 14 has two possible		
30′	337.5	329.4	-1.1	conformations: extended and hydrogen-bonded. The extended acidity					

Information.

Scheme 1. Gas Phase Acidity of Imidazoles

337.7

338.0

31

32

330.1

331.0

4.7

5.1

-CN, -CF₃, and -CH₃. Their acidity decreases with the trend: 4 > 6' > 13 > 19 > 54, where 4 is the most acidic. This is consistent with the substitution patterns. Likewise, for the 2-substituted imidazoles, the acidity trend is as follows: 5 > 10 > 12 > 18 > 56, where substituents are, respectively, -SO₂Cl, -NO₂, -CN, -CF₃, and -CH₃.

 $\Delta H^{\circ}_{rxn} = \Delta H^{\circ}_{acid}; \ \Delta G^{\circ}_{rxn} = \Delta G^{\circ}_{acid}$

Gas-Phase Acidity: Experiments. While calculations are valuable, the accuracy of any chosen method and level is always in question. We did calculate the acidity of the parent, unsubstituted imidazole as well; its computed ΔG°_{acid} of 342.1 kcal/mol compares favorably to the experimental value of 342.6 kcal/mol.³⁴ To further benchmark some of our

calculated values, we measured imidazole gas-phase acidity. We utilized acidity bracketing in a Fourier transform mass spectrometer. We selected imidazoles by computations represented a range in acidity. Proton transfer reactions between reference acids whose acidities are known and the conjugate base of the imidazoles, as well as the reverse reaction, were tracked. The presence or absence of proton transfer was assessed.

is listed here; the acidity value for the hydrogen-bonded structure is

slightly less, 318.2 kcal/mol. Details are in the Supporting

The results are shown in Tables 2 and 3. Column "a' represents the reaction between the conjugate base of the imidazole and the neutral reference acid. Column "b" represents the reaction between the deprotonated reference acid and the neutral imidazole. For imidazole 9, the conjugate base of 9 cannot deprotonate 1,1,1-trifluoro-2,4-pentadione $(\Delta^{\circ}_{acid} = 322.0 \text{ kcal/mol})$, but 1,1,1-trifluoro-2,4-pentadione enolate can deprotonate 9. The conjugate base of 9 deprotonates trifluoroacetic acid ($\Delta G^{\circ}_{acid} = 317.4 \text{ kcal/mol}$), but the reverse reaction does not take place. We therefore bracket imidazole 9 to have a ΔG°_{acid} of 320 \pm 4 kcal/mol. Imidazole 11 reacts the same as 9; thus 11 has a ΔG°_{acid} also of 320 \pm 4 kcal/mol. The conjugate base of 13 cannot extract a proton from difluoroacetic acid ($\Delta G^{\circ}_{acid} = 323.8 \text{ kcal/mol}$); however, difluoroacetate is basic enough to abstract a proton from 13. The conjugate base of 13 is basic enough to proton transfer from 3,5-bis(trifluoromethyl)phenol ($\Delta G^{\circ}_{acid} = 322.9$ kcal/mol), but the reverse reaction does not occur, placing the

Table 2. Summary of Results for Gas-Phase Acidity Bracketing of Imidazoles 9, 11, 13, 19, 34, and 38

		proton transfer ^{b,c}											
		-	9	1	.1	1	.3	1	9	3	4	3	88
reference acid	acidity a (ΔG°_{acid} , kcal/mol)	a	b	a	b	a	ь	a	b	a	b	a	ь
formic acid	339.2 ± 1.5											-	+
acetylacetone	336.7 ± 2.0									_	+	_	+
methyl cyanoacetate	334.5 ± 2.0									_	+	_	+
trifluoro-m-cresol	332.4 ± 2.0							_	+	+	_	+	_
pyruvic acid	326.5 ± 2.8					_	+	_	+	+	_	+	_
difluoroacetic acid	323.8 ± 2.0	_	+	_	+	_	+	+	_				
3,5-bis(trifluoromethyl)phenol	322.9 ± 2.0	_	+	_	+	+	_	+	_				
1,1,1-trifluoro-2,4-pentadione	322.0 ± 2.0	_	+	_	+	+	_						
trifluoroacetic acid	317.4 ± 2.0	+	_	+	_								
3,5-bis(trifluoromethyl)pyrazole	317.3 ± 2.0	+	_	+	_								

[&]quot;Reference 35. "The "+" symbol indicates the occurrence of proton transfer, and the "-" symbol indicates the absence of proton transfer. c"a" represents the reaction between the deprotonated imidazole and the neutral reference acid; "b" represents the reaction between the deprotonated reference acid and the neutral imidazole.

Table 3. Summary of Results for Gas-Phase Acidity Bracketing of Imidazoles 40, 41, 46, 49, and 56

		proton transfer b,c									
		4	10	4	1	4	6	4	.9	5	56
reference acid	acidity a ($\Delta G^\circ_{ m acid}$, kcal/mol)	a	ь	a	ь	a	b	a	ь	a	ь
2-propanethiol	347.1 ± 2.0							_	+	_	+
1-pentanethiol	346.2 ± 2.5							_	+	_	+
p-cresol	343.4 ± 2.0							_	+	+	_
acetic acid	341.1 ± 2.0							+	_	+	_
butyric acid	339.5 ± 2.0			_	+	_	+	+	_	+	_
formic acid	339.2 ± 1.5	-	+	_	+	_	+	+	_		
acetylacetone	336.7 ± 2.0	_	+	_	+	_	+				
methyl cyanoacetate	334.5 ± 2.0	_	+	+	_	+	_				
trifluoro-m-cresol	332.4 ± 2.0	+	_	+	_	+	_				
pyruvic acid	326.5 ± 2.8	+	_								

[&]quot;Reference 35. b"The "+" symbol indicates the occurrence of proton transfer, and the "-" symbol indicates the absence of proton transfer. c"a" represents the reaction between the deprotonated imidazole and the neutral reference acid; "b" represents the reaction between the deprotonated reference acid and the neutral imidazole.

 ΔG°_{acid} of 13 at 323 \pm 3 kcal/mol. Pyruvate (ΔG°_{acid} = 326.5 kcal/mol) can deprotonate 19, while the reverse reaction does not occur. The conjugate base of 19 can deprotonate difluoroacetic acid ($\Delta G^{\circ}_{acid} = 323.8 \text{ kcal/mol}$), but difluoroacetate is not basic enough to deprotonate 19. We place the ΔG°_{acid} of 19 to be 326 \pm 4 kcal/mol. For 34, 38, and 40, the deprotonated imidazoles do not react with methyl cyanoacetate ($\Delta G^{\circ}_{acid} = 334.5 \text{ kcal/mol}$), but deprotonated methyl cyanoacetate can deprotonate 34, 38, and 40. The conjugate base of all three imidazoles can abstract a proton from trifluoro-m-cresol ($\Delta G^{\circ}_{acid} = 332.4 \text{ kcal/mol}$), but the cresolate does not deprotonate the imidazoles, placing the acidity for 34, 38, and 40 at 333 \pm 3 kcal/mol. The reaction of deprotonated 41 and acetylacetone ($\Delta G^{\circ}_{acid} = 336.7 \text{ kcal/mol}$) does not result in proton transfer; however, the reverse reaction between 41 and acetylacetone enolate does result in proton transfer. The conjugate base of 41 does deprotonate methyl cyanoacetate ($\Delta G^{\circ}_{acid} = 334.5 \text{ kcal/mol}$), but the reverse reaction does not occur, placing the ΔG°_{acid} of 41 at 336 \pm 3 kcal/mol. Imidazole 46 reacts the same as 41, so its acidity is also 336 ± 3 kcal/mol. For imidazole 49, the reaction between the conjugate base and p-cresol ($\Delta G^{\circ}_{acid} = 343.4 \text{ kcal/mol}$) does not occur, but the reverse reaction does. Acetate (ΔG°_{acid} = 341.1. kcal/mol) cannot deprotonate 49, but the conjugate base of 49 can deprotonate acetic acid. We therefore bracket 49 to 342 \pm 3 kcal/mol. The conjugate base of 56 cannot transfer a proton from 1-pentanethiol (($\Delta G^{\circ}_{acid} = 346.2 \text{ kcal/mol}$), but 1-pentanethiolate can deprotonate 56. The conjugate base of 56 can deprotonate *p*-cresol (($\Delta G^{\circ}_{acid} = 343.4 \text{ kcal/mol}$); the reverse reaction does not occur. The ΔG°_{acid} of imidazole 56 is therefore 345 \pm 4 kcal/mol.

Computational versus Experimental Results. A summary of the computational and experimental results is shown in Table 4 and Figure 2. For the computational data, if an imidazole has more than one possible tautomer, the acidity of the most stable tautomer is listed first. As noted earlier, a "prime" mark next to the structure number indicates the 5-substituted imidazole structure.

There is general agreement between the calculated acidity of the more stable tautomer, and the experimentally determined values, thus benchmarking the calculations (Figure 2). The basicity of the anionic component of the AHA ILs for carbon dioxide capture is important and often assessed by calculation, but gas-phase data to which those computed values can be directly compared is generally scarce. Our experiments therefore help fill this knowledge gap.

Tautomers. One interesting possibility arising from these studies is the ability to ascertain whether a less stable tautomer

Table 4. Calculated (B3LYP/6-311++G(d,p); 298 K) and Experimental Gas-Phase Acidity Values for Imidazoles^a

substrate	calculated $\Delta G^{\circ}_{ m acid}$ more stable/less stable tautomer	experimental $\Delta G^{\circ}_{ m acid}$
9	318.2	320 ± 4
11	319.6 (11')/318.5 (11)	320 ± 4
13	321.3 (13)/321.1 (13')	323 ± 2
19	325.9 (19)/324.7 (19')	326 ± 4
34	331.2 (34)/330.1 (34')	333 ± 3
38	332.2 (38')/329.2 (38)	333 ± 3
40	332.4 (40)/330.7 (40')	333 ± 3
41	333.9	336 ± 3
46	335.0 (46)/333.5 (46')	336 ± 3
49	342.4	342 ± 3
56	343.3	345 ± 4
^a Values ar	e in kcal/mol.	

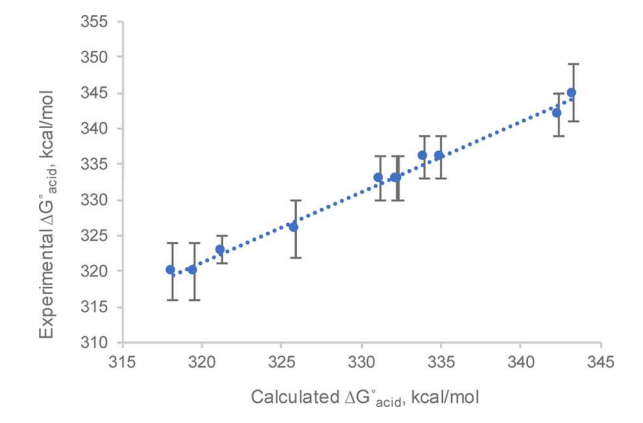


Figure 2. Plot of experimental $\Delta G^{\circ}_{\text{acid}}$ versus calculated $\Delta G^{\circ}_{\text{acid}}$ (acidity of more stable tautomer used). Equation for the line: y = 0.986x + 5.687; $R^2 = 0.991$.

is present under our conditions. If two tautomers are different enough in energy, their acidities will be different, and measurement of acidity could potentially be used to assess the structure. For example, the 5-substituted tautomer 38′ is more stable than the 4-substituted tautomer 38, by 3 kcal/mol. This difference is reflected in the calculated acidity difference (332.2 kcal/mol for 38′ and 329.2 kcal/mol for 38).

Our acidity bracketing experiment involves running two reactions: the conjugate base of the reference acid with the imidazole and the imidazolate with the reference acid. These are run separately, not at equilibrium (see Experimental Section for details). The predicted behavior if one or both tautomers is present is shown in Figure 3. Direction "a" corresponds to the reaction of the conjugate base of 38 and a reference acid HA. The conjugate base of 38 is the same as the conjugate base of 38'. Since the most basic site of this anion has a calculated $\Delta G^{\circ}_{\text{acid,calc}}$ of 332.2 kcal/mol, the reaction would be expected to occur with any HA that has a $\Delta G^{\circ}_{
m acid}$ of about 332 kcal/mol or lower. In the opposite direction, "b", two scenarios are possible. If only the most stable tautomer 38' is present, then the conjugate base of the reference acid HA (A⁻) would need to be basic enough to deprotonate the N-H $(\Delta G^{\circ}_{\text{acid,calc}} = 332.2 \text{ kcal/mol})$. However, if both tautomers 38' and 38 are present, a different proton transfer pattern will be seen. Since 38 has a $\Delta G^{\circ}_{acid,calc}$ of 329.2 kcal/mol, proton transfer would be expected to occur as long as the conjugate

base of the reference acid has a ΔG°_{acid} of at least ~329 kcal/mol.

The resultant hypothetical bracketing table is shown in Table 5. The first and second columns (a and b) indicate the expected results if both the more stable 38' and less stable 38 structures were present. If neutral 38 (calculated acidity = 329.2 kcal/mol) were present, then trifluoro-*m*-cresolate ($\Delta^{\circ}_{\text{acid,expt}}$ = 332.4 kcal/mol) and trifluoro-*p*-cresolate ($\Delta G^{\circ}_{\text{acid,expt}}$ = 330.1 kcal/mol) would be expected to deprotonate it ("+" in column b). The third and fourth columns (a and b) show our actual observations. The "-" in column b for trifluoro-*m*-cresolate ($\Delta G^{\circ}_{\text{acid,expt}}$ = 332.4 kcal/mol) and trifluoro-*p*-cresolate ($\Delta G^{\circ}_{\text{acid,expt}}$ = 330.1 kcal/mol) makes it unlikely that the more acidic, less stable tautomer 38 ($\Delta G^{\circ}_{\text{acid,calc}}$ = 329.2 kcal/mol) is present. Our results indicate that only 38' is present. Thus, under our gas-phase conditions, the major structure is the 5-substituted tautomer 38', which is consistent with our computational prediction.

Acidity and Carbon Dioxide Absorption. Prior studies have indicated that for ionic liquids with heterocyclic anions that capture carbon dioxide, the basicity of the anionic nucleophile (which is also the acidity of the nucleophile's conjugate acid) is important for tuning CO₂ absorption capacity. ^{1,13,15,19–30}

To assess carbon dioxide capture, we computed the free energy of the reaction shown in eq 1, for our 56 imidazoles.

Prior studies have shown that the carbamate-type structure in eq 1 is the product of CO_2 capture. We plotted the ΔG°_{rxn} for eq 1 versus computed imidazole acidity. The gasphase data are in Table 1, and the resultant plot is shown in Figure 4. 21

There is a rough linear correlation between the ΔG° of formation of the imidazolate—carbon dioxide complex and the acidity of the imidazole. The less acidic the imidazole (i.e., the more basic the imidazolate), the more exergonic the complexation reaction shown in eq 1. This result shows promise for the design/choice of imidazolates for CO_2 capture; our studies have benchmarked the calculations and show that the more basic anions yield more stable CO_2 adducts.

We also calculated the acidity of the 56 imidazoles in an ionic liquid medium. Prior work has indicated that calculations in the solvent may be more relevant than gas-phase computations for ionic liquid-based carbon dioxide capture systems. ^{22,27} Ji, Cheng and co-workers, in a recent study relating IL anion basicity to CO₂ absorption capacity, assessed anion basicity in the ionic liquid [DBUH⁺][OTf⁻]; we likewise used [DBUH⁺][OTf⁻] as a model. ²² The resultant plot is shown in Figure 5 (detailed calculational data in the Supporting Information). This plot shows a better linear correlation than in the gas phase, and again, the more basic imidazolates correspond to more favorable carbon dioxide complexation.

As noted earlier when we discussed imidazole acidity, the less basic imidazolates are generally substituted with more electron-withdrawing groups. Another observation is that substitution on the 2-position renders the addition of CO_2 less exergonic than substitution on the 4-position (CO_2 adducts shown in Figure 6). Table 6 lists imidazole pairs



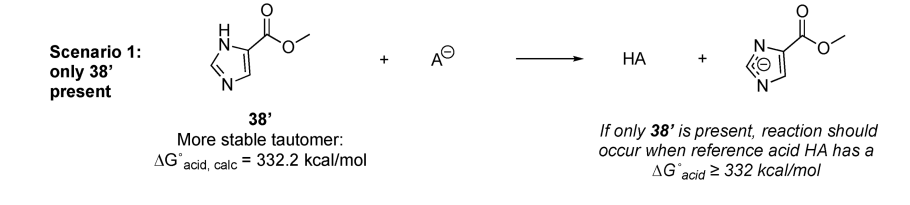
conjugate base of 38: no tautomeric structures

This anion should deprotonate any HA with
$$\Delta G^*_{acid} \leq 332 \ kcal/mol$$

$$A \ominus + HA$$

$$A \ominus + H$$

Direction "b": two scenarios



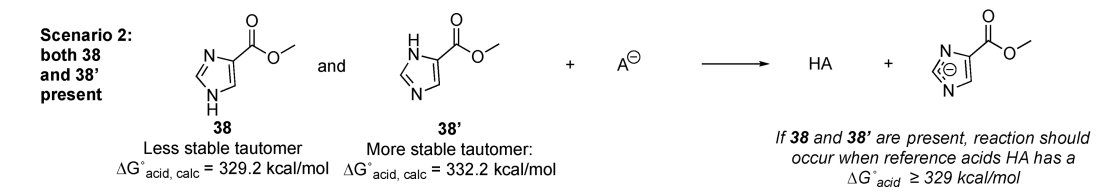


Figure 3. Possible bracketing pathways for 38/38'.

Table 5. Expected Bracketing Results if 38 and 38' Are both Present (Figure 3)

		pr	proton transfer ^{b,c}			
		resu 38' 38	ected lts if and are sent		ual ults	
reference acid	$\operatorname{acidity}^{a}\left(\Delta G^{\circ}_{\operatorname{acid}},\operatorname{kcal/mol}\right)$	a	ь	a	ь	
formic acid	339.2 ± 1.5	-	+	-	+	
acetylacetone	336.7 ± 2.0	_	+	-	+	
methyl cyanoacetate	334.5 ± 2.0	_	+	-	+	
trifluoro-m-cresol	332.4 ± 2.0	+	+	+	_	
trifluoro-p-cresol	330.1 ± 2.0	+	+	+	_	
pyruvic acid	326.5 ± 2.8	+	_	+	_	

"Reference 35. "The "+" symbol indicates the occurrence of proton transfer, and the "-" symbol indicates the absence of proton transfer. "a" represents the reaction between the deprotonated imidazole and the neutral reference acid; "b" represents the reaction between the deprotonated reference acid and the neutral imidazole.

that have the same substituent but on the 2-position versus the 4-position. The calculated ΔG°_{rxm} for the addition of carbon dioxide in ionic liquid is also listed for each pair. The imidazolates that produce 4-substituted CO_2 adducts all have a more exergonic reaction than the 2-substituted analogues. The 4-substituted imidazolates are in general more basic than the 2-substituted imidazolates, but the differences in basicity are not as great as the differences in CO_2 adduct exergonicity; for example, deprotonated 4 is 4.8 kcal/mol, more basic than deprotonated 5, but the difference in the ΔG° of CO_2 complexation is 10.6 kcal/mol (Table 6). The greater exergonicity for the 4-substituted substrates is consistent with experimental observations; 2-substituted imidazole-based ILs have generally lower CO_2 capacities than 4-substituted

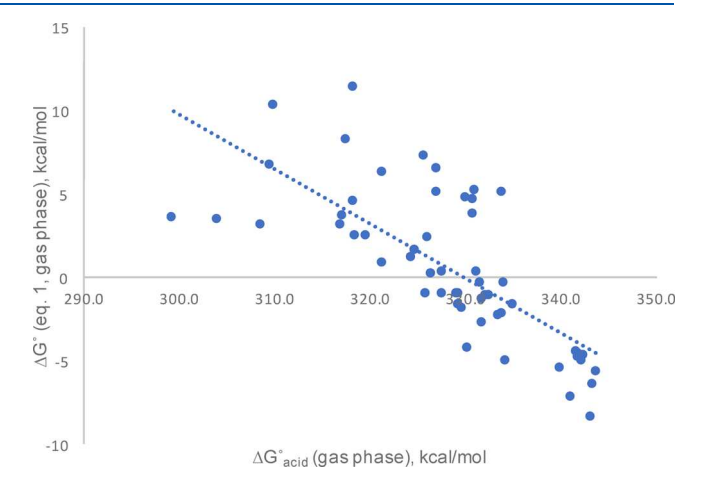


Figure 4. Relationship between calculated gas-phase ΔG°_{ran} for eq 1 and the calculated gas-phase $\Delta G^{\circ}_{acid,calc}$ of imidazoles. Equation for the line: y = -0.328x + 108.07; $R^2 = 0.545$.

ILs. 31 One preliminary theory concerning this difference in reactivity was proposed by Zhu and co-workers, who noted that a substituent on the 2-position could present steric hindrance to the addition of carbon dioxide to the adjacent nitrogen anion. 31 Steric effects are typically kinetic, but our calculations indicate that there is a thermochemical preference for the formation of CO_2 adducts with the substituent at the 4-position. The issue is most probably also steric; an adduct with carbon dioxide would certainly be expected to be more sterically crowded and less stable with substitution on the 2-position versus the 4-position (Figure 6).

Overall, our results are consistent with prior work also showing correlations between basicity of the nucleophile and ${\rm CO_2}$ complexation in ionic liquids. $^{1,13,15,16,18-30}$ Furthermore, Firaha et al. observed that if the computed OCO angle (in a

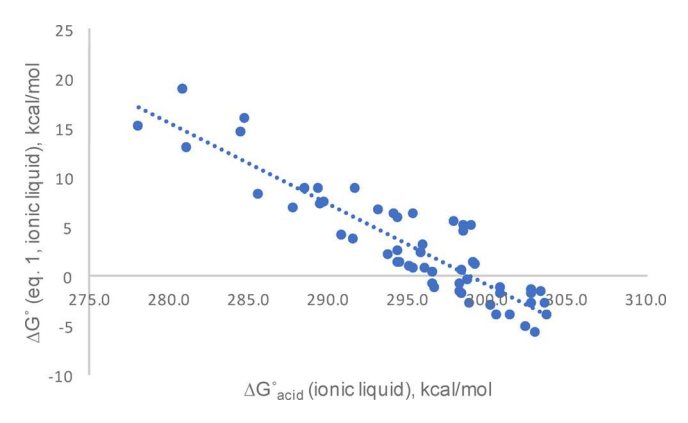


Figure 5. Relationship between $\Delta G^{\circ}_{\text{rxn}}$ for eq 1 and $\Delta G^{\circ}_{\text{acid,calc}}$ of imidazoles in ionic liquid. Equation for the line: y = -0.820x + 245.02; $R^2 = 0.824$.

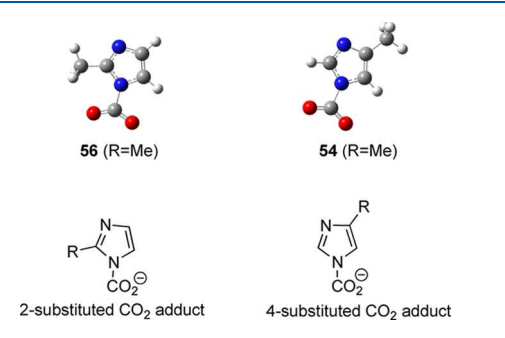


Figure 6. Structures for the 2-substituted CO_2 adduct and the 4-substituted CO_2 adduct. Calculated structures for **56** and **54** are shown as representative examples.

solvent dielectric of 15) is less than 140°, then chemical absorption (nucleophilic reaction between the anion and carbon dioxide) is likely to occur. Our results are consistent with this study, in that the OCO angle in ionic liquids is calculated to be less than 140° for all our substrates (detailed data in the Supporting Information). These authors also predict that promising anions for IL capture have calculated ΔG°_{rxn} values (in a medium of dielectric 15) ranging from roughly -7 to +4 kcal/mol. As can be seen in Figure 5, should this prediction be valid, many of the imidazolates described herein are promising candidates for carbon dioxide capture.

Ultimately, our study is the first to examine a wide range of imidazolates, with experimental gas-phase measurements that indicate the accuracy of the calculations. Carbon dioxide capture and storage is a matter of urgency, and our data herein will help in the understanding of the relationship between basicity of imidazolates and chemical absorption of imidazolate-containing ILs.

CONCLUSIONS

In this work, 56 imidazoles are examined both computationally and experimentally. These data are relevant for the improved design and tuning of anion-based ionic liquids for carbon dioxide capture. The measurements are the first for these substrates and benchmark the calculations. A linear correlation is found between imidazole acidity and the free energy of reaction for anion- CO_2 association, which is improved when an ionic liquid computational model is used. The results show the tunability of imidazolates for carbon dioxide capture.

EXPERIMENTAL SECTION

All the experimentally measured imidazoles are commercially available and were used without further purification.

Acidity bracketing measurements were conducted using a Fourier transform ion cyclotron resonance mass spectrometer (FTMS) with a dual cell setup, which has been described previously. $^{39-46}$ The magnetic field is 3.3 T; the baseline pressure is 1×10^{-9} Torr. The imidazoles, which are solids, were volatilized into the cell via a heatable solid probe, while the reference acids were introduced via a system of heatable batch inlets or leak valves. Water was pulsed into the cell and ionized by an electron beam (typically 8 eV, 9 μ A, 0.5 s) to generate hydroxide ions. The reactions between the imidazoles and reference acids were measured in both directions, in separate experiments. In one direction, the imidazolate anions were generated by the reaction of the imidazoles with the hydroxide ions. The imidazolate anions were then selected and transferred from one cubic cell to another via a 2 mm hole in the middle trapping plate. Transferred ions were cooled with pulsed argon gas that allowed the pressure to raise to 10⁻⁵ Torr. The reaction with the reference acid was then tracked. In the opposite direction, the conjugate bases of the reference acid were generated by the reaction with hydroxide. These anions were then transferred to the second cell to react with neutral imidazoles. Experiments were conducted at ambient temperature. The typical protocol for obtaining gas-phase rate constants has been described previously. 39,40,43,44,47 The experiments are run under pseudo-first-order conditions with the neutral reactant in excess, relative to the reactant anions. Reading the pressure of the neutral compounds from the ion gauges is not always accurate; therefore, we "back out" the neutral substrate pressure from fast control reactions (described previously). 39,42,43,45,48,49

All calculations were performed using the density functional theory (B3LYP/6-311++G(d,p)) as implemented in Gaussian $16.^{50-54}$ All ground state geometries were fully optimized, and frequencies were calculated for both gas-phase and solvation calculations; no scaling factor was applied. The optimized structures had no negative frequencies. For the solvation calculations, the solvation model density (SMD) method was

Table 6. Calculated (B3LYP/6-31++G(d,p) ΔG°_{rxn} for CO₂ Addition for 2-Substituted and 4-Substituted Imidazole Pairs in Ionic Liquid

functional group	2-substituted structure number/ ΔG° for CO_2 addition in IL	4-substituted structure number/ ΔG° for CO_2 addition in IL	Is 4-substituted more exergonic?/By how many kcal/mol?
-SO ₂ Cl	5/+18.8 kcal/mol	4/+8.2 kcal/mol	yes/10.6 kcal/mol
$-NO_2$	10/+15.9 kcal/mol	6 /+6.8 kcal/mol	yes/9.1 kcal/mol
-CN	12/+7.1 kcal/mol	13/+3.7 kcal/mol	yes/3.4 kcal/mol
$-CF_3$	18/+8.6 kcal/mol	19/+2.0 kcal/mol	yes/6.6 kcal/mol
$-CH_3$	56 /-2.8 kcal/mol	54 /-5.2 kcal/mol	yes/2.4 kcal/mol

used with ionic liquid [DBUH][OTf] as the solvent. The solvent descriptors for [DBUH][OTf] were derived based on the "SMD-GIL" method developed by Contreras, Cramer, Truhlar and co-workers (details in the Supporting Information). The temperature for the calculations was set to be 298 K.

ASSOCIATED CONTENT

S Supporting Information

The Supporting Information is available free of charge on the ACS Publications website at DOI: 10.1021/acs.joc.9b02193.

Cartesian coordinates and further details for all calculated species (PDF)

AUTHOR INFORMATION

Corresponding Author

*E-mail: jee.lee@rutgers.edu.

ORCID ®

Jeehiun K. Lee: 0000-0002-1665-1604

Notes

The authors declare no competing financial interest.

ACKNOWLEDGMENTS

We thank the NSF and the NSF Extreme Science and Engineering Discovery Environment (XSEDE) for support.

REFERENCES

- (1) Cui, G.; Wang, J.; Zhang, S. Active chemisorption Sites in Functionalized Ionic Liquids for Carbon Capture. *Chem. Soc. Rev.* **2016**, *45*, 4307–4339.
- (2) Bates, E. D.; Mayton, R. D.; Ntai, I.; Davis, J. H. CO₂ Capture by a Task-Specific Ionic Liquid. *J. Am. Chem. Soc.* **2002**, 124, 926–927.
- (3) Boot-Handford, M. E.; Abanades, J. C.; Anthony, E. J.; Blunt, M. J.; Brandani, S.; Mac Dowell, N.; Fernández, J. R.; Ferrari, M.-C.; Gross, R.; Hallett, J. P.; Haszeldine, R. S.; Heptonstall, P.; Lyngfelt, A.; Makuch, Z.; Mangano, E.; Porter, R. T. J.; Pourkashanian, M.; Rochelle, G. T.; Shah, N.; Yao, J. G.; Fennell, P. S. Carbon Capture and Storage Update. *Energy Environ. Sci.* 2014, 7, 130–189.
- (4) MacDowell, N.; Florin, N.; Buchard, A.; Hallett, J.; Galindo, A.; Jackson, G.; Adjiman, C. S.; Williams, C. K.; Shah, N.; Fennell, P. An Overview of CO₂ Capture Technologies. *Energy Environ. Sci.* **2010**, *3*, 1645–1669.
- (5) Yang, Z.-Z.; Zhao, Y.-N.; He, L.-N. CO₂ Chemistry: Task-Specific Ionic Liquids for CO₂ Capture/Activation and Subsequent Conversion. *RSC Adv.* **2011**, *1*, 545–567.
- (6) Bara, J. E.; Camper, D. E.; Gin, D. L.; Noble, R. D. Room-Temperature Ionic Liquids and Composite Materials: Platform Technologies for CO₂ Capture. *Acc. Chem. Res.* **2010**, *43*, 152–159.
- (7) Huang, J.; Rüther, T. Why are Ionic Liquids Attractive for CO₂ Absorption? An Overview. Aust. J. Chem. 2009, 62, 298–308.
- (8) Zhao, Z.; Dong, H.; Zhang, X. The Research Progress of CO₂ Capture with Ionic Liquids. *Chin. J. Chem. Eng.* **2012**, 20, 120–129.
- (9) Zhang, X.; Zhang, X.; Dong, H.; Zhao, Z.; Zhang, S.; Huang, Y. Carbon Capture with Ionic Liquids: Overview and Progress. *Energy Environ. Sci.* **2012**, *5*, 6668–6681.
- (10) Ramdin, M.; de Loos, T. W.; Vlugt, T. J. H. State-of-the-Art of CO₂ Capture with Ionic Liquids. *Ind. Eng. Chem. Res.* **2012**, *51*, 8149–8177.
- (11) Zhang, J.; Zhang, S.; Dong, K.; Zhang, Y.; Shen, Y.; Lv, X. Supported Absorption of CO₂ by Tetrabutylphosphonium Amino Acid Ionic Liquids. *Chem. Eur. J.* **2006**, *12*, 4021–4026.
- (12) Zhang, Y.; Zhang, S.; Lu, X.; Zhou, Q.; Fan, W.; Zhang, X. Dual Amino-Functionalised Phosphonium Ionic Liquids for CO₂ Capture. *Chem. Eur. J.* **2009**, *15*, 3003–3011.

- (13) Wang, C.; Luo, X.; Luo, H.; Jiang, D.-e.; Li, H.; Dai, S. Tuning the Basicity of Ionic Liquids for Equimolar CO₂ Capture. *Angew. Chem. Int. Ed.* **2011**, *50*, 4918–4922.
- (14) Gutowski, K. E.; Maginn, E. J. Amine-Functionalized Task-Specific Ionic Liquids: A Mechanistic Explanation for the Dramatic Increase in Viscosity upon Complexation with CO₂ from Molecular Simulation. *J. Am. Chem. Soc.* **2008**, *130*, 14690–14704.
- (15) Wang, C.; Luo, H.; Jiang, D.-e.; Li, H.; Dai, S. Carbon Dioxide Capture by Superbase-Derived Protic Ionic Liquids. *Angew. Chem. Int. Ed.* **2010**, *49*, 5978–5981.
- (16) Seo, S.; Quiroz-Guzman, M.; DeSilva, M. A.; Lee, T. B.; Huang, Y.; Goodrich, B. F.; Schneider, W. F.; Brennecke, J. F. Chemically Tunable Ionic Liquids with Aprotic Heterocyclic Anion (AHA) for CO₂ Capture. *J. Phys. Chem. B* **2014**, *118*, 5740–5751.
- (17) Seo, S.; DeSilva, M. A.; Xia, H.; Brennecke, J. F. Effect of Cation on Physical Properties and CO_2 Solubility for Phosphonium-Based Ionic Liquids with 2-Cyanopyrrolide Anions. *J. Phys. Chem. B* **2015**, *119*, 11807–11814.
- (18) Gurkan, B.; Goodrich, B. F.; Mindrup, E. M.; Ficke, L. E.; Massel, M.; Seo, S.; Senftle, T. P.; Wu, H.; Glaser, M. F.; Shah, J. K.; Maginn, E. J.; Brennecke, J. F.; Schneider, W. F. Molecular Design of High Capacity, Low Viscosity, Chemically Tunable Ionic Liquids for CO₂ Capture. *J. Phys. Chem. Lett.* **2010**, *1*, 3494–3499.
- (19) Lei, X.; Xu, Y.; Zhu, L.; Wang, X. Highly Efficient and Reversible CO₂ Capture through 1,1,3,3-Tetramethylguanidinium Imidazole Ionic Liquid. *RSC Adv.* **2014**, *4*, 7052–7057.
- (20) Wang, C.; Luo, X.; Zhu, X.; Cui, G.; Jiang, D.-e.; Deng, D.; Li, H.; Dai, S. The Strategies for Improving Carbon Dioxide Chemisorption by Functionalized Ionic Liquids. *RSC Adv.* **2013**, *3*, 15518–15527
- (21) Wang, Z.; Wang, F.; Xue, X.-S.; Ji, P. Acidity Scale of N-Heterocyclic Carbene Precursors: Can We Predict the Stability of NHC-CO₂ Adducts? *Org. Lett.* **2018**, *20*, 6041–6045.
- (22) Gao, F.; Wang, Z.; Ji, P.; Cheng, J.-P. CO₂ Absorption by DBU-Based Protic Ionic Liquids: Basicity of Anion Dictates the Absorption Capacity and Mechanism. *Frontiers in Chemistry* **2019**, *6*, 658.
- (23) Wang, C.; Luo, H.; Li, H.; Zhu, X.; Yu, B.; Dai, S. Tuning the Physicochemical Properties of Diverse Phenolic Ionic Liquids for Equimolar CO₂ Capture by the Substituent on the Anion. *Chem. Eur. J.* **2012**, *18*, 2153–2160.
- (24) Venkatraman, V.; Gupta, M.; Foscato, M.; Svendsen, H. F.; Jensen, V. R.; Alsberg, B. K. Computer-aided molecular design of imidazole-based absorbents for CO₂ capture. *Int. J. Greenhouse Gas Control* **2016**, 49, 55–63.
- (25) Zhao, T.; Zhang, X.; Tu, Z.; Wu, Y.; Hu, X. Low-viscous Diamino Protic Ionic Liquids with Fluorine-Substituted Phenolic Anions for Improving ${\rm CO_2}$ Reversible Capture. *J. Mol. Liq.* **2018**, 268, 617–624.
- (26) Vijayraghavan, R.; Pas, S. J.; Izgorodina, E. I.; MacFarlane, D. R. Diamino Protic Ionic Liquids for CO₂ Capture. *Phys. Chem. Chem. Phys.* **2013**, *15*, 19994–19999.
- (27) Firaha, D. S.; Hollóczki, O.; Kirchner, B. Computer-Aided Design of Ionic Liquids as CO₂ Absorbents. *Angew. Chem. Int. Ed.* **2015**, *54*, 7805–7809.
- (28) Sudha, S. Y.; Khanna, A. Evaluating the Interactions of CO₂-Ionic Liquid Systems through Molecular Modeling. *World Acad. Sci., Eng. Tech. Int. J. Chem. Molec. Eng.* **2009**, *3*, 524–527.
- (29) Bhargava, B. L.; Balasubramanian, S. Insights into the Structure and Dynamics of a Room-Temperature Ionic Liquid: Ab Initio Molecular Dynamics Simulation Studies of 1-n-Butyl-3-methylimidazolium Hexafluorophosphate ([bmim][PF₆]) and the [bmim][PF₆]-CO₂ Mixture. *J. Phys. Chem. B* **2007**, 111, 4477–4487.
- (30) Ren, S.; Hou, Y.; Tian, S.; Chen, X.; Wu, W. What are Functional Ionic Liquids for the Absorption of Acidic Gases? *J. Phys. Chem. B* **2013**, *117*, 2482–2486.
- (31) Zhu, X.; Song, M.; Xu, Y. DBU-Based Protic Ionic Liquids for CO2Capture. ACS Sustainable Chem. Eng. 2017, 5, 8192–8198.
- (32) We note that Alsberg and co-workers²⁴ calculated and measured the pK_a in water of a series of imidazoles while we cannot

- compare our values directly with theirs; since we did not calculate pK_a , we do find a clear linear relationship between his pK_a values and our ΔG°_{acid} values in water (plot in the Supporting Information).
- (33) We note that we calculated the acidity of the NH_2 on structure 8, which might be expected to be somewhat acidic. We find that the NH_2 site is more than 10 kcal/mol, less acidic than the NH imidazole site.
- (34) Linstrom, P. J.; Mallard, W. G. NIST Chemistry WebBook, NIST Standard Reference Database Number 69., National Institute of Standards and Technology, Gaithersburg MD, 20899, http://webbook.nist.gov, (retrieved 2019).
- (35) Kaljurand, I.; Koppel, I. A.; Kütt, A.; Rõõm, E.-I.; Rodima, R.; Koppel, I.; Mishima, M.; Leito, I. Experimental Gas-Phase Basicity Scale of Superbasic Phosphazenes. *J. Phys. Chem. A* **2007**, *111*, 1245–50
- (36) Pan, M.; Cao, N.; Lin, W.; Luo, X.; Chen, K.; Che, S.; Li, H.; Wang, C. Reversible CO₂ Capture by Conjugated Ionic Liquids through Dynamic Covalent Carbon-Oxygen Bonds. *ChemSusChem* **2016**, *9*, 2351–2357.
- (37) Luo, X.; Guo, Y.; Ding, F.; Zhao, H.; Cui, G.; Li, H.; Wang, C. Significant Improvements in CO2Capture by Pyridine-Containing Anion-Functionalized Ionic Liquids through Multiple-Site Cooperative Interactions. *Angew. Chem. Int. Ed.* **2014**, *53*, 7053–7057.
- (38) The linear correlation is slightly better ($R^2 = 0.679$) when calculated ΔH° values are used (see the Supporting Information for plot); this may reflect an issue with the gas-phase entropy computation.
- (39) Kurinovich, M. A.; Lee, J. K. The Acidity of Uracil from the Gas Phase to Solution: The Coalescence of the N1 and N3 Sites and Implications for Biological Glycosylation. *J. Am. Chem. Soc.* **2000**, *122*, 6258–6262.
- (40) Kurinovich, M. A.; Phillips, L. M.; Sharma, S.; Lee, J. K. The Gas Phase Proton Affinity of Uracil: Measuring Multiple Basic Sites and Implications for the Enzyme Mechanism of Orotidine 5′-monophosphate Decarboxylase. *Chem. Comm.* **2002**, 2354–2355.
- (41) Sharma, S.; Lee, J. K. Acidity of Adenine and Adenine Derivatives and Biological Implications. A Computational and Experimental Gas-Phase Study. *J. Org. Chem.* **2002**, *67*, 8360–8365.
- (42) Sun, X.; Lee, J. K. Acidity and Proton Affinity of Hypoxanthine in the Gas Phase versus in Solution: Intrinsic Reactivity and Biological Implications. *J. Org. Chem.* **2007**, *72*, 6548–6555.
- (43) Liu, M.; Li, T.; Amegayibor, F. S.; Cardoso, D. S.; Fu, Y.; Lee, J. K. Gas-Phase Thermochemical Properties of Pyrimidine Nucleobases. *J. Org. Chem.* **2008**, *73*, 9283–9291.
- (44) Liu, M.; Xu, M.; Lee, J. K. The Acidity and Proton Affinity of the Damaged Base 1,N⁶-Ethenoadenine in the Gas Phase versus in Solution: Intrinsic Reactivity and Biological Implications. *J. Org. Chem.* **2008**, 73, 5907–5914.
- (45) Zhachkina, A.; Liu, M.; Sun, X.; Amegayibor, F. S.; Lee, J. K. Gas-Phase Thermochemical Properties of the Damaged BaseO6-Methylguanine versus Adenine and Guanine. *J. Org. Chem.* **2009**, *74*, 7429–7440.
- (46) Sharma, S.; Lee, J. K. Gas-Phase Acidity Studies of Multiple Sites of Adenine and Adenine Derivatives. *J. Org. Chem.* **2004**, *69*, 7018–7025.
- (47) Kurinovich, M. A.; Lee, J. K. The Acidity of Uracil and Uracil Analogs in the Gas Phase: Four Surprisingly Acidic Sites and Biological Implications. J. Am. Soc. Mass Spectrom. 2002, 13, 985–995.
- (48) Chesnavich, W. J.; Su, T.; Bowers, M. T. Collisions in a Noncentral Field: A Variational and Trajectory Investigation of Ion-Dipole Capture. *J. Chem. Phys.* **1980**, *72*, 2641–2655.
- (49) Su, T.; Chesnavich, W. J. Parametrization of the Ion-Polar Molecule Collision Rate Constant by Trajectory Calculations. *J. Chem. Phys.* **1982**, *76*, 5183–5185.
- (50) Lee, C.; Yang, W.; Parr, R. G. Development of the Colle-Salvetti Correlation-Energy Formula into a Functional of the Electron Density. *Phys. Rev. B* **1988**, *37*, 785–789.
- (51) Becke, A. D. Density-Functional Thermochemistry. III. The Role of Exact Exchange. *J. Chem. Phys.* **1993**, *98*, 5648–5652.

I

- (52) Becke, A. D. A New Mixing of Hartree-Fock and Local Density-Functional Theories. J. Chem. Phys. 1993, 98, 1372–1377.
- (53) Stephens, P. J.; Devlin, F. J.; Chabalowski, C. F.; Frisch, M. J. Ab Initio Calculation of Vibrational Absorption and Circular Dichroism Spectra Using Density Functional Force Fields. *J. Phys. Chem.* **1994**, 98, 11623–11627.
- (54) Frisch, M. J.; Trucks, G. W.; Schlegel, H. B.; Scuseria, G. E.; Robb, M. A.; Cheeseman, J. R.; Scalmani, G.; Barone, V.; Petersson, G. A.; Nakatsuji, H.; Li, X.; Caricato, M.; Marenich, A. V.; Bloino, J.; Janesko, B. G.; Gomperts, R.; Mennucci, B.; Hratchian, H. P.; Ortiz, J. V.; Izmaylov, A. F.; Sonnenberg, J. L.; Williams-Young, D.; Ding, F.; Lipparini, F.; Egidi, F.; Goings, J.; Peng, B.; Petrone, A.; Henderson, T.; Ranasinghe, D.; Zakrzewski, V. G.; Gao, J.; Rega, N.; Zheng, G.; Liang, W.; Hada, M.; Ehara, M.; Toyota, K.; Fukuda, R.; Hasegawa, J.; Ishida, M.; Nakajima, T.; Honda, Y.; Kitao, O.; Nakai, H.; Vreven, T.; Throssell, K.; Montgomery, J. A., Jr.; Peralta, J. E.; Ogliaro, F.; Bearpark, M. J.; Heyd, J. J.; Brothers, E. N.; Kudin, K. N.; Staroverov, V. N.; Keith, T. A.; Kobayashi, R.; Normand, J.; Raghavachari, K.; Rendell, A. P.; Burant, J. C.; Iyengar, S. S.; Tomasi, J.; Cossi, M.; Millam, J. M.; Klene, M.; Adamo, C.; Cammi, R.; Ochterski, J. W.; Martin, R. L.; Morokuma, K.; Farkas, O.; Foresman, J. B.; Fox, D. J. Gaussian 16, Rev. B.01. Gaussian, Inc.: Wallingford CT, 2016.
- (55) Bernales, V. S.; Marenich, A. V.; Contreras, R. H.; Cramer, C. J.; Truhlar, D. G. Quantum Mechanical Continuum Solvation Models for Ionic Liquids. *J. Phys. Chem. B* **2012**, *116*, 9122–9129.